First International Conference on Damage Tolerance of Aircraft Structures
R. Benedictus, J. Schijve, R.C. Alderliesten, J.J. Homan (Eds.)

DETERMINATION OF THE FATIGUE CRACK-GROWTH RATES FROM FRACTOGRAPHIC ANALYSIS OF SPECIMENS REPRESENTING AIRCRAFT WING SKIN

Marcin Ciesielski[*], Jerzy Kaniowski[**], Włodzimierz Karliński[**]

[*] Materials Engineers Group Ltd
141 Wołoska St. 02-507 Warsaw, Poland
e-mail: m.ciesielski@megrop.pl
[**] Institute of Aviation, New Technology Center, Aircraft Department
Al. Krakowska 110/114, 02-256 Warsaw, Poland
e-mail: jerzy.kaniowski@ilot.edu.pl, wlodzimierz.karlinski@ilot.edu.pl

Abstract. *This paper presents an example of the macroscopic and microscopic fractographic analysis of an aircraft structure component fatigue tested in laboratory conditions. The program loading was derived from a load spectrum representing the realistic in-service conditions. The fatigue crack growth rates determined from the fatigue striations have been related to the number of flights. The presented results refer to stable crack propagation in the aircraft wing skin.*

1. INTRODUCTION

Determination of the crack growth rate for real loads allows us to define safe aircraft service life after fracture detection and the period and range of the maintenance required.

In the Institute of Aviation, a wide program of fatigue tests and analyses based on safe-life methodology for PZL I-22 training and combat jet aircraft airframe has been carried out. The fractures in wing skin structure specimens have been examined fractographicaly with an aim to determine the crack initiation origins and fatigue crack-growth rate.

1. FATIGUE TEST

The subject of the fractographic examination was a specimen of the lower wing skin, previously subjected to fatigue test [1]. The specimen structure is presented in fig. 2, and the loading history in fig. 1. Specimen after the fatigue tests is presented in fig. 3a.

Specimen skin and the doubler were manufactured from D16CzATV aluminium alloy (of Russian origin and 2124-Alclad as American counterpart), double plated and anodized. Skin and doubler were cut from the 4 mm gauge plate in such a way, that direction of applied loads was parallel to plate rolling direction. The skin has been locally etched on the internal side, up to 2 mm thickness. Stringer spacing were 115 mm. Stringers were manufactured from extruded aluminum PA33 (2014) alloy angle.

As the test log [2], recorded during the specimen tests, stringer **1** was damaged the first (see fig. 3b), in the place of the M6 bolt hole. After 386 400 load cycles, the crack was detected during inspection preceding application of **7A** (ascending) loads step block (see load history in fig.

1), i.e. after 161 load blocks. Afterwards, skin cracks in the plane of four rivets, joining skin with doubler, were observed. Crack description in the report was as follows: crack running from the specimen edge with the stringer intact (stringer **2** in fig. 3b) to the distance 15 mm from the last rivet, then the crack runs through the row of three rivet holes (fig. 3a). This condition was observed during the next inspection, after 604 800 cycles (252 load blocks), during inspection preceding **7A** step load series of the next loads block. Damage of the skin as a result of fatigue crack propagation took place after 608 397 cycles (253 load blocks) during loads in the second cycle of **1A** step, in the 254th load block.

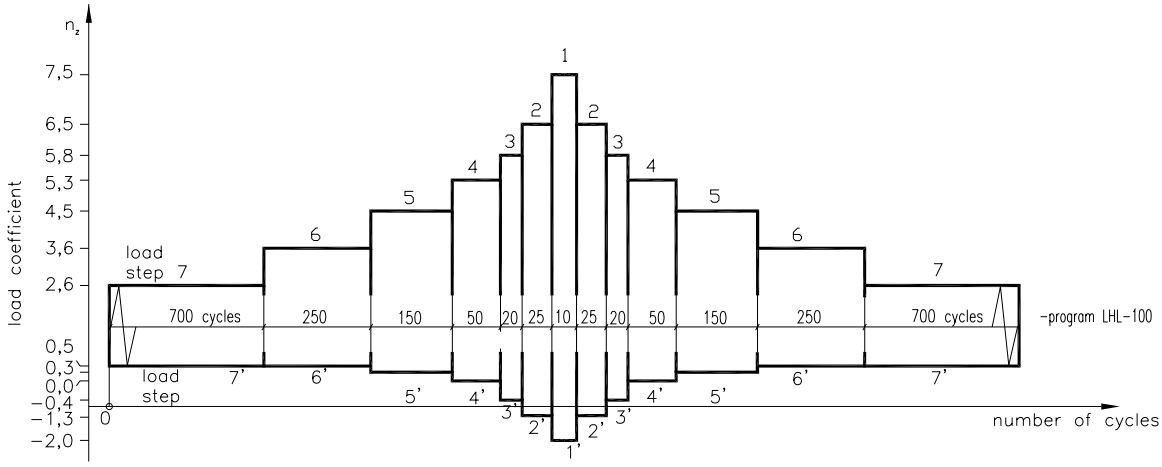

Fig. 1. Loading history of the specimen during fatigue test[2]. The loads were applied in blocks, corresponding to 100 flights; the sequence of loads were from low to high to low within each block.

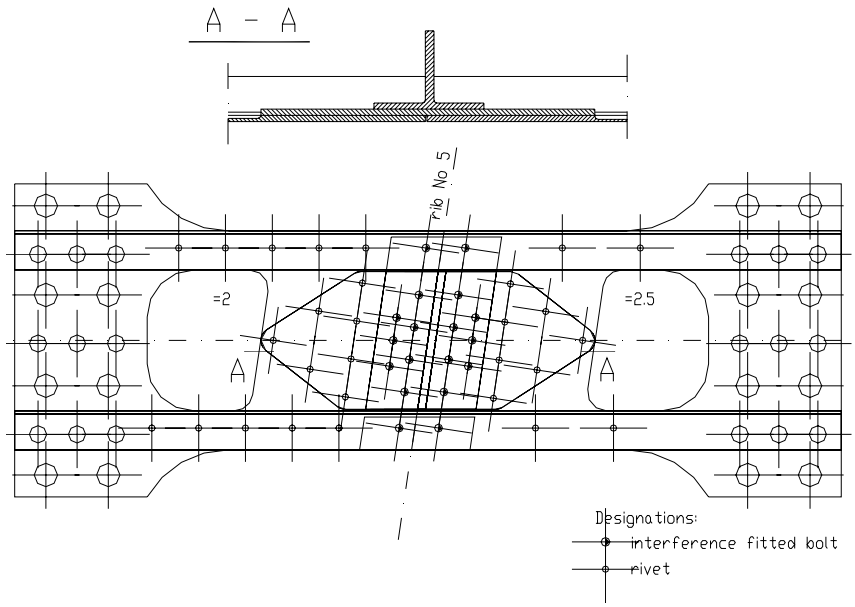

Fig. 2. Fragment of the lower wing skin specimen.

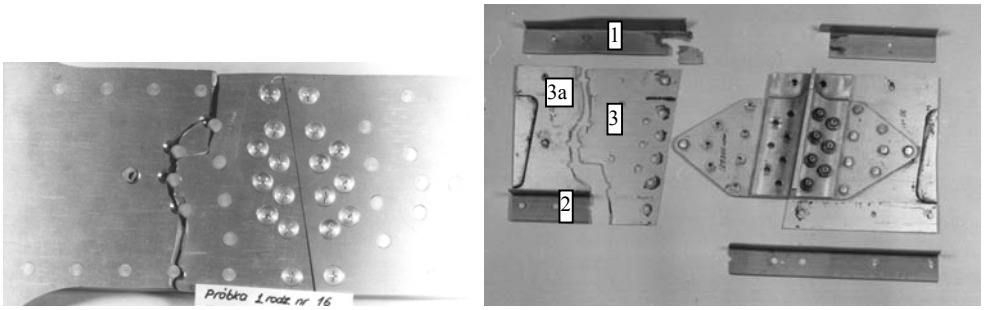

a) b)

Fig. 3. The appearance of the specimen after the test (a) and its elements (b) after partial disassembly. Designations: **1** and **2** - stringers, **3** and **3a** - skin.

2. ANALYSIS OF THE SKIN FRACTURE

The analysis included fractures of the skin and both stringers. Distinct crack-growth bands were seen at the fatigue fracture of the skin. The fatigue fracture of the stringer **1** had no visible crack-growth bands, whereas fracture of the stringer **2** was of static type [3]. Skin crack goes along a broken line, crosswise through rivet holes. A fragment of the skin with a crack has been shown in fig. 4. Respective rivets were designated with numbers from **1** to **5**. Rivets 1 to 4 joins the skin with the doubler, rivet **5** joins the skin with the stringer. Respective fatigue sections of the fracture were designated with letters **A** to **F**. Length of the respective sections and the numbers of fatigue crack-growth bands are given in table 1. In some sections the fatigue fracture one cannot distinguish fatigue crack-growth bands. Their length has not been added to the length of the sections.

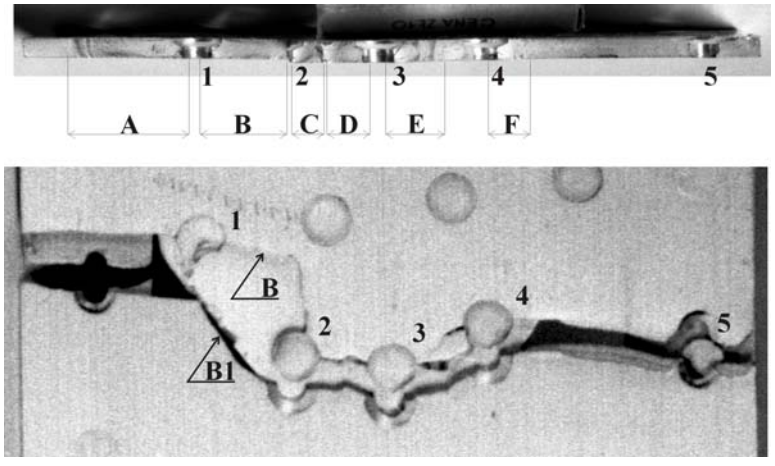

Fig. 4. Fracture and the position of skin crack. Numbers designate the rivet holes and letters refer to the fracture sections.

On the basis of macrofractographic analysis one can conclude that the initiation of the skin crack occurred in hole **1** on both of its sides (sections **A** and **B** in fig. 5). Fracture **A** propagated to the edge of the specimen, while fracture **B** from the other side of the hole **1**

propagated to the rivet hole **2** in figure 4. The longest fatigue crack bands segment among all segments of the fracture confirmed that the cracking process started at hole **1** of the wing skin. The initiation of all the crack segments took place in the rivet holes. It was also observed that the cracks propagated from both sides of the holes and met between the holes as it is shown in figure 6 (segments **C** and **D** between holes **2** and **3**) or passed by as it occurred e.g. between holes **1** and **2** or **3** and **4**. Whereas, on the basis of the hitherto test one cannot determine in what order cracks were initiated from the successive holes.

No.	Section designation	Section length in mm	Count of the crack-growth bands
1	A	22,3	42
2	B	17,7	54
4	C	6,2	20
5	D	6,8	18
6	E	8,1	12
7	F	4,9	11

Table 1. Fatigue fracture sections characteristics.

After the macroscopic analysis of all fragments it was decided to determine crack growth rate within a stable crack growth range, starting at stage I of fatigue (initiation). Fig. 5 shows a fragment of the fracture being subject of the a.m. tests.

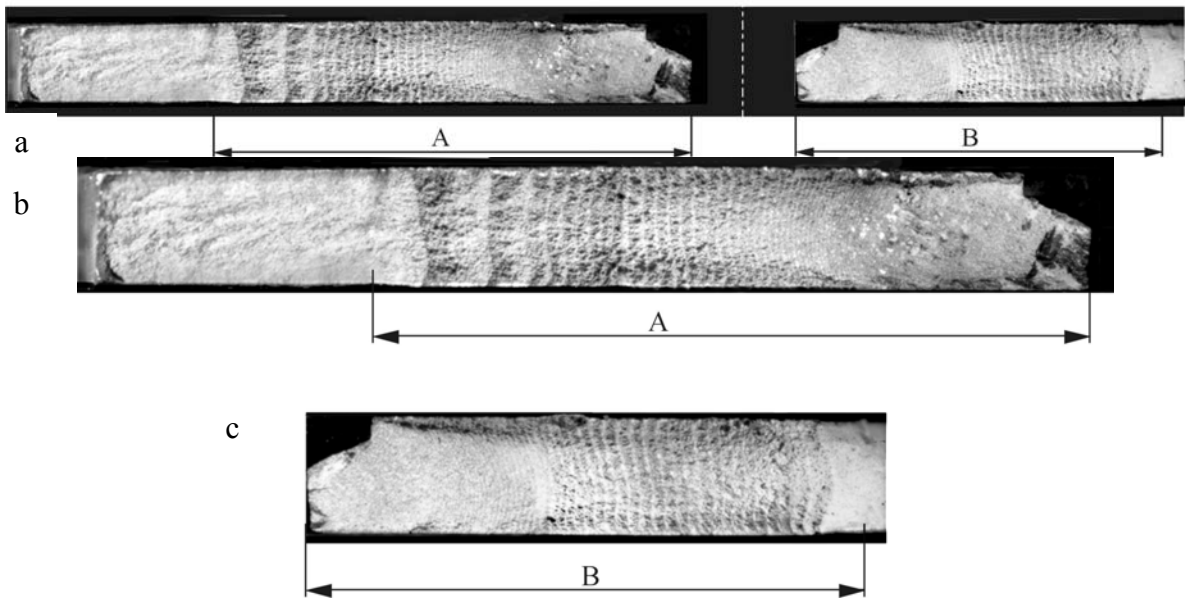

Fig. 5. Designations of fatigue sections of the wing skin specimen fracture for which of fatigue-growth bands have been counted, a – the appearance of the sections A and B of the fracture, b and c segments for which CGR was determined.

3. DETERMINING THE CRACK-GROWTH RATE

On the basis of macrofractographic analysis an attempt has been made to estimate fatigue crack-growth rate [4]. The crack length has been determined by measuring the distance from the crack initiation hole to the farthest fatigue crack-growth band and the distance between successive fatigue growth-bands (sections A and B in figure 6). It is known that fracture crack-growth bands correspond to the maximal stresses realized in the load block[5]. Therefore, relation of crack length growth in the function of load blocks count can be determined.

In the case of section **A** (fig. 5) the initiation of the fatigue crack started in hole **1** (fig. 4). In figure 5 distinct fatigue crack-growth bands can be seen. Fatigue origins are shown in figure 6. The standard methodology of microscopic examination was used. Only departure from the standard was choosing grains with crack direction identical with macroscopic crack instead of statistical measurements of crack growth rate in particular grains. On the surface of the hole traces of rivet interference were seen. At the distance of about 2 mm from the origin, the first blocks of fatigue striations have been observed (fig. 7). As it is shown in the figure, ten fatigue striations correspond to the step **1** (S1) of the load history, while 25 fatigue striations correspond to the step **2A** (S2).

At the distance of about 4 mm from the origin, blocks of wider fatigue striations can be seen, what indicates an increase of crack-growth rate. On the enlarged figure 8, the wider fatigue striations correspond to step **1** of the load history, while 25 fatigue striations correspond to step **2A** (S2). It was also seen that fatigue striations, which belong to the same load step have various widths and various directions, what testifies to different crack-growth rate in various grains of the material tested.

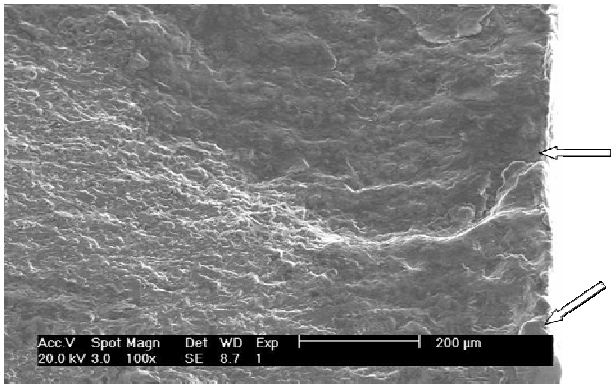

Fig. 6. Fatigue origins and fatigue zone in **A** section, near the hole **1**. Two fatigue origins near the rivet hole can be seen.

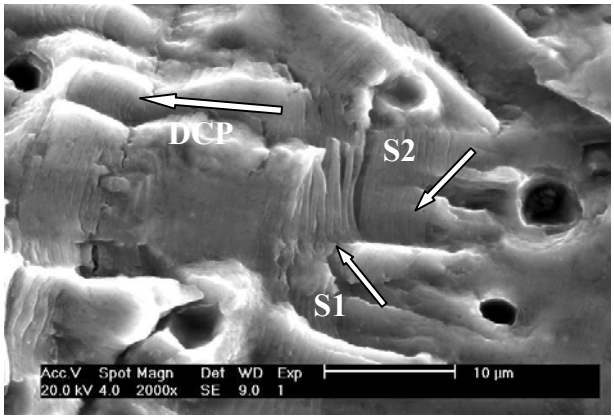

Fig. 7. Fatigue striations on the fracture of the specimen section **A**, at the distance of about 2 mm from the hole. **DCP** – direction of crack propagation, **S1** – step **1** of the load, **S2** – step **2** of the load.

Farther from the origin, group of striations with higher spacing than these at distance of about 4 mm from the origin has been observed, what confirms the increase of crack-growth rate. The group of striations corresponding to step **1** of the load history is about 50 μm wide. In figure 9, group of striations, which corresponds to steps **2** and **3**, is shown.

On the graph, fig. 10, crack-growth rate relation to the distance from the edge of the hole is shown.

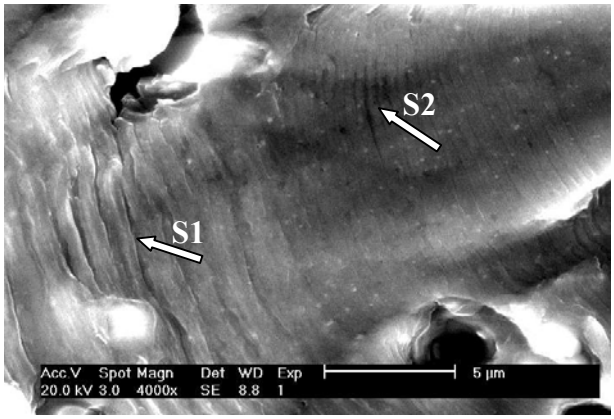

Fig. 8. Fatigue striations on the section **A** at the distance of about 4 mm from edge of the hole.

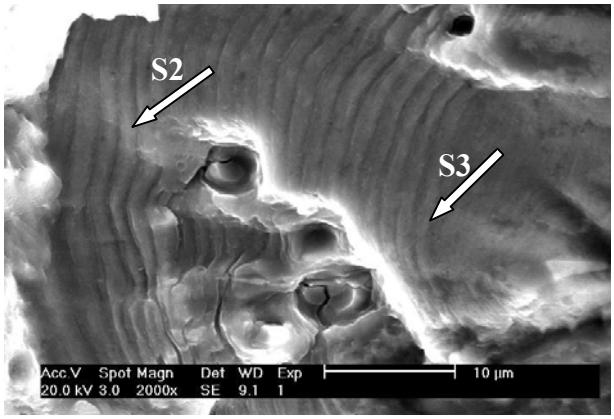

Fig. 9. Fatigue striations on the section **A** at the distance of about 14 mm from edge of the hole.

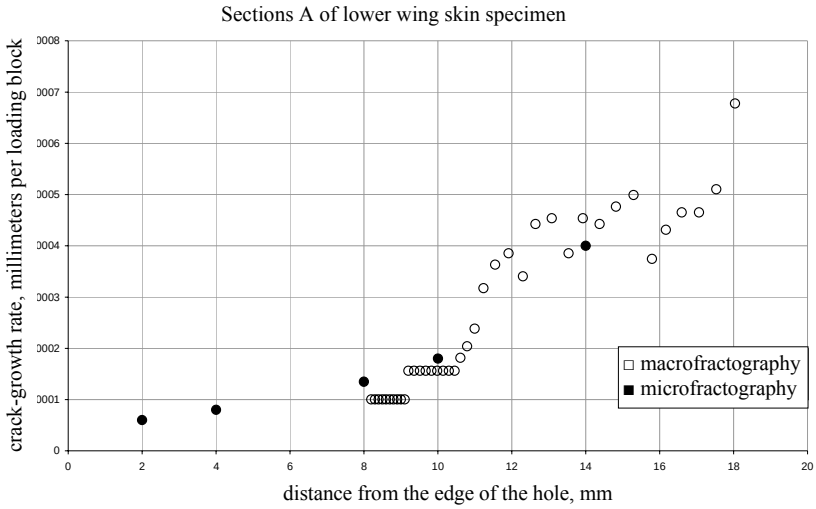

Fig. 10. Crack-growth rate for the fragment **A** of the wing lower skin specimen fracture.

Next element on which fractographic analysis and identification with load history was performed is the section **B** of the fracture, shown in figure 4. In this case, the initiation of the fatigue crack also took place on the edge of the hole **1** (fig. 5). The appearance of the fatigue striations is similar to the ones in the section **A**.

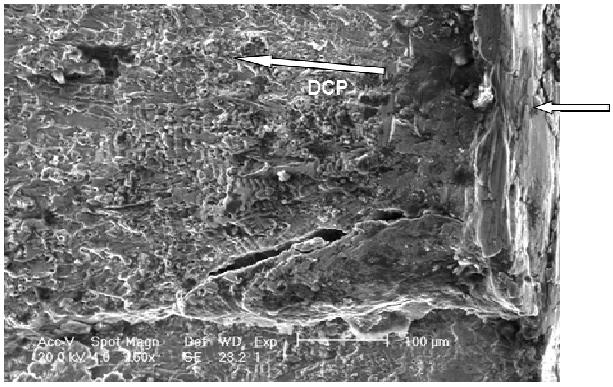

Fig. 11. Fatigue origins and fatigue zone in section **B**, near the hole **1**.

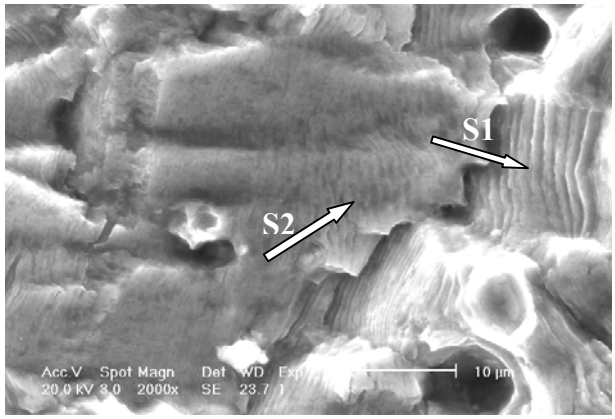

Fig. 12. Fatigue striations in the **B** section of the fracture, at the distance of about 2 mm from edge of the hole. Designations show the group of 10 striations corresponding to the step **1** of the load (arrow S1**)** and 25 striations corresponding to the step **2A** of the load (arrow S2**)**.

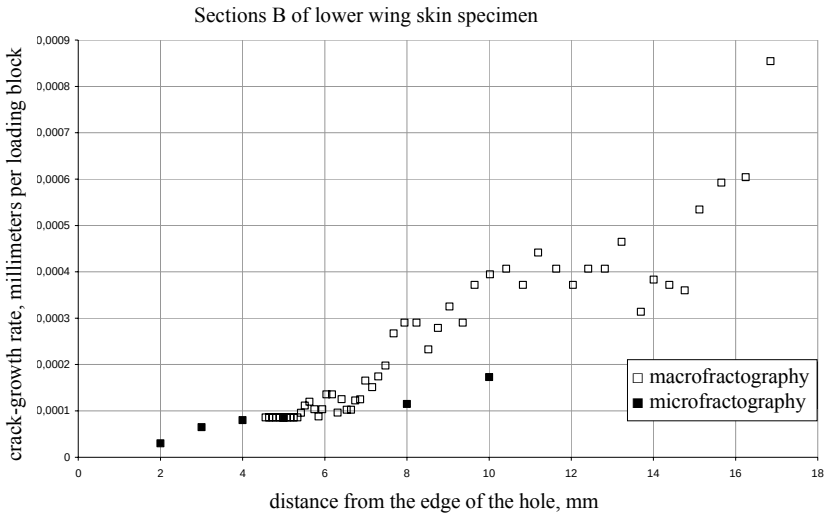

Fig. 13. Crack-growth rates for section **B** of the wing lower skin specimen fracture.

On the basis of the examinations for sections **A** and **B** of the fracture, relation of the crack-growth rate (expressed in millimetres per load history block) to ΔK has been determined (fig. 14).

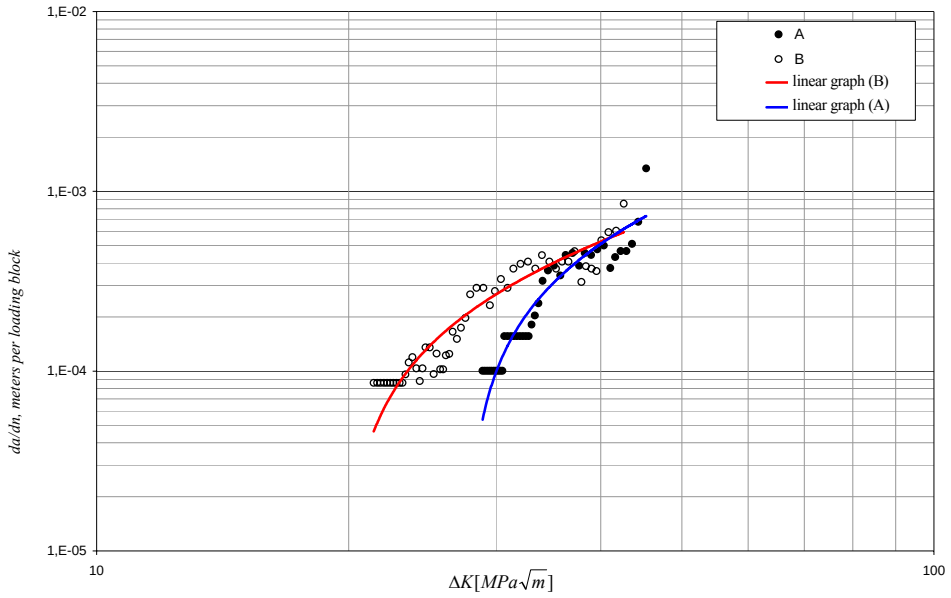

Fig. 14. Relation of the crack-growth rate to ΔK for the sections **A** and **B**.

4. CONCLUSIONS

Determining the crack growth-rate in standard laboratory specimens (for testing of crack growth speed) poses no problems with experiments, as the place of its propagation is preceded with a notch and a pre-crack. To fulfil such a task on a construction specimen, and even more on a real object, is quite difficult due to the fact that one can never know where the crack initiation appears. Crack propagation monitoring makes also some problems, because the crack covers the distance between the rivet holes in a short period of time, holes that are the places of initiating and hindering the cracking process.

In the graphs (fig. 10 and 13) the results of macroscopic and microscopic measurements have been presented. The application of the microscopic method, based on selection of crack-growth rate measurement in these grains where direction of crack precisely corresponds with the macroscopic direction, caused that the microscopic measurements in initial stage of cracking were exact extension of both graphs in the direction of the origin. Further crack propagation proceeds differently. Two questions arise here: (1) why macroscopic and microscopic crack growth rates agrees at the **A** section (fig. 10) and (2) why they differ significantly at the **B** section (fig. 13)? As it is known, fatigue striations are forming on the slip planes [6, p.85]. Microfractograms of the section **A** (figs. 8 and 9) show a great number of plateaus and relatively small number of dimples, containing inclusions. The plateaus correspond to the surface area of the fracture created as a result of plastic slip deformation, and dimples show the plastic deformations according to the pore coagulation mechanism. The latter type of plastic deformation is characteristic for overload and static cracks. On the fatigue fractures, overload zones occur during passage to next load blocks and during the breaking stage. Mixed fractures (dimples plus fatigue striations) are typical for damage,

occurring at stresses cyclic intensity being close to the value K_{1C} of metal [6, p. 74]. The photography of the section **B** (fig. 12) shows a smaller number of plateaus and a greater number of dimples than on the section **A**. It is the result of specimen stresses increase after **A** fracture.

While the crack-growth rate determined from the spacing between the fatigue striations concerns only the plastic slip mechanism, the macroscopic rate covers both processes: plastic slip and micro-pore coagulation, causing that it is almost always higher than the microscopic rate [6]. In this case, contribution of the dimple fracture in section **A** is relatively small and the estimated values of microscopic and macroscopic crack-growth rates are similar. However, in section **B** contribution of dimple fracture is crucial, so the difference between rates is essential.

Plastic slip deformation occurs at lower stresses than deformation by micro-pore coagulation. Considering this, dimples count on the section **B** is greater, because of the specimen stresses increase in result of the crack growth, resulting in decrease of specimen cross section.

It seems, that in the case of crack-growth rate measurements in real structures, e.g. for expertise purposes, macroscopic measurements are more useful, as the results are closer to the real crack-growth rate and the method is much less labour consuming.

Traditional measurement methods would require a great number of crack propagation gages. This would be expensive, due to their high cost. Presented results of the research show that the applied method allows estimating the crack-growth rate. Obtaining full information on the tested wing skin crack-growth rate requires performing a microfractographic analysis related with loading history [7] and using MES modelling for determining accurate results of stresses spread. Such research program is being planned.

REFERENCES

[1] J. Kaniowski: *Realizacja badań zmęczeniowych fragmentów struktury płatowca samolotu W-300*. Niepublikowane sprawozdanie Instytutu Lotnictwa nr 50/BW-W1/86, grudzień 1986. (*Carrying out research on fatigue fragments of airframe structures for W-300 aircraft.* Unpublished report of the Institute of Aviation No 50/BW, December 1986.).

[2] J. Kaniowski: *Badania wpływu geometrycznych cech konstrukcyjnych na trwałość zmęczeniową na przykładzie skrzydła samolotu PZL I-22*. Rozprawa doktorska, Akademia Techniczno-Rolnicza w Bydgoszczy, 1998. (*The Study of the Geometric Features Influence on the Fatigue Durability at the Plane Wing Case.* PhD Thesis, University of Technology and Agriculture in Bydgoszcz, 1998.).

[3] E. Dorn: *Wyniki badań nr 15/BM-1/89*, kwiecień 1989. (*Research Results No 15/BM-1/89,* April 1989.).

[4] M. Ciesielski, W. Karliński, J. Kaniowski: *Analiza mechanizmu pękania skrzydła na podstawie badań mikro i makrofraktograficznych.* Niepublikowane sprawozdanie Instytutu Lotnictwa, listopad 2003. Praca wykonana w ramach projektu badawczego nr 7T07B00419, sfinansowanego przez Komitet Badań Naukowych. (*An analysis of the wing cracking mechanism on the basis of micro- and macrofractographic research.*

Unpublished report of the Institute of Aviation, November 2003. The work prepared as part of the research project no. 7T07B00419, financed by the State Committee for Science Research).

[5] R. W. Hertzberg: *Deformation and fracture mechanics of engineering materials.* John Willey & sons, New York 1989, p. 459.

[6] Metals Handbook, 8th edition, „*Fraktography and Atlas Fractogramus*", ASM 1974.

[7] J. Schijve: *The significance of fractography for investigation of fatigue crack growth under variable-amplitude loading*. Fatigue Fract. Engng. Mater. Struct., Vol. 22, pp. 87-99.